Published as: *Nature*. 2012 August 9; 488(7410): 226–230.

Programmed elimination of cells by caspase-independent cell extrusion in *C. elegans*

Daniel P. Denning, **Victoria Hatch**, and **H. Robert Horvitz**
Howard Hughes Medical Institute and Department of Biology, Massachusetts Institute of Technology, Cambridge, MA 02139

Abstract

The elimination of unnecessary or defective cells from metazoans occurs during normal development and tissue homeostasis as well as in response to infection or cellular damage[1]. While many cells are removed through caspase-mediated apoptosis followed by phagocytosis by engulfing cells[2], other mechanisms of cell elimination occur[3], including the extrusion of cells from epithelia via a poorly understood, possibly caspase-independent process[4]. Here we identify a mechanism of cell extrusion that is caspase-independent and that can eliminate a subset of the *Caenorhabditis elegans* cells programmed to die during embryonic development. In wild-type animals, these cells die soon after their generation via caspase-mediated apoptosis. However, in mutants lacking all four *C. elegans* caspase genes, these cells nonetheless are eliminated by being extruded from the developing embryo into the extra-embryonic space of the egg. The shed cells exhibit apoptosis-like cytological and morphological characteristics, indicating that apoptosis can occur in the absence of caspases in *C. elegans*. We describe a kinase pathway required for cell extrusion involving PAR-4, STRD-1 and MOP-25.1/2, the *C. elegans* homologs of the mammalian tumor suppressor kinase LKB1 and its binding partners STRADα and MO25α. The AMPK-related kinase PIG-1, a possible target of the PAR-4:STRD-1:MOP-25 kinase complex, is also required for cell shedding. PIG-1 promotes shed cell detachment by preventing the cell surface expression of cell-adhesion molecules. Our findings reveal a mechanism for apoptotic cell elimination fundamentally distinct from that of canonical programmed cell death.

Keywords

asymmetric cell division; cell polarity; excretory cell

The CED-3 caspase is essential for nearly all programmed cell deaths that occur during *C. elegans* development[5]. However, a few cells undergo programmed cell death in *ced-3* mutants[5–7]. We observed that some cells are eliminated from *ced-3* embryos by being shed from the developing animal. The eggs of *ced-3* mutants but not those of wild-type animals contained on average six shed cells that had detached during the comma stage of

Author contributions:
D.P.D. and H.R.H. designed the experiments, analyzed the data and wrote the manuscript.
D.P.D. and V.H. performed the experiments.

embryogenesis (~300 minutes post fertilization) (Figs. 1a–c and f; Supplemental Table S1). The shed cells detached at the anterior sensory depression or the ventral pocket (Figs. 2a–b) and remained within the egg (but separate from the animal) throughout embryogenesis. Embryos with a loss-of-function mutation in the *Apaf-1* homolog *ced-4* or the BH3 domain-encoding gene *egl-1* or a gain-of-function mutation of the *bcl-2* homolog *ced-9* also produced shed cells (Fig. 1c), indicating that a defect in any step of the execution phase of programmed cell death can generate shed cells. As reported previously[8], mutant embryos defective in engulfment (e.g., *ced-1* or *ced-5* embryos) contain "floaters" (Figs. 1c–d and g; Supplemental Table S1), cells that undergo CED-3-mediated apoptosis and detach from the embryo because they cannot be internalized by engulfing cells. In comparison to *ced-3* shed cells, *ced-5* floaters were smaller, more uniformly refractile when viewed by Nomarski optics, and less likely to aggregate into clumps of three or more cells after detachment (Figs. 1a–b and d; Supplemental Table S1). *ced-3* mutations were epistatic to engulfment mutations with respect to the number of shed cells, their appearance, and their tendency to aggregate (Supplemental Table S1; data not shown). Thus, the shed cells of embryos defective in programmed cell death are genetically and morphologically distinguishable from those of embryos defective in engulfment.

The *C. elegans* genome encodes three additional caspase homologs: *csp-1*, *csp-2* and *csp-3*[9]. We determined that individual *csp* mutations did not cause the appearance of shed cells (Supplemental Fig. S1; Supplemental Table S2). Eggs from quadruple mutants lacking all four caspase genes, like *ced-3* eggs, contained on average six shed cells (Figs. 1c and e), indicating that the generation of shed cells is caspase independent.

Although caspase activation can drive apoptosis, recent studies have suggested that caspases are not necessary for apoptosis[3]. We therefore examined *csp-3; csp-1; csp-2 ced-3* (*csp*-Δ) shed cells for apoptotic characteristics, specifically phosphatidylserine (PS) exposure and TUNEL (terminal deoxynucleotidyl transferase dUTP nick end labeling)-reactive DNA fragments. Like floaters that undergo caspase-mediated apoptosis (Supplemental Fig. S2; ref. 8), the *csp*-Δ shed cells were reactive to the PS-binding protein MFG-e8 and to TUNEL staining (Figs. 1h–i). Also, *ced-3* shed cells exhibited chromatin condensation (darkly staining nuclear material) and separation of the nuclear envelope double membrane in transmission electron micrographs (Fig. 1f and Supplemental Fig. S3). These apoptotic features were present in *ced-5* floaters (Fig. 1g and Supplemental Fig. S3), although the cytoplasms of *ced-5* floaters were more compact. We conclude that the shed cells of embryos lacking caspase activity are in many respects cytologically and morphologically apoptotic, indicating that caspases are dispensable for many cellular changes that occur during apoptosis.

The somatic cell lineage of *C. elegans* is essentially invariant[10,11], allowing the precise identification of cell origins and fates. To determine the cellular identities of *ced-3* shed cells, we recorded time-lapse videos of developing *ced-3* embryos and traced the lineages of extruded cells in reverse (Figs. 2a–b; Supplemental Movie S1). We identified seven different cells eliminated by shedding from *ced-3* embryos (Fig. 2c), all of which are cells that normally die during wild-type embryogenesis. This finding is consistent with our observation that *ced-3* shed cells expressed *egl-1* (Fig. 2d), the transcription of which

initiates programmed cell death[12], and with a previous report in which ABalapapaa (a cell fated to die) was observed detaching from a *ced-3* embryo[5]. The cells that can be shed are among the first to die in the wild-type embryo: 14 cells die within the first 300 minutes of development, and seven of the eight identified shed cells are among this group of 14 cells[11]. Thus, specific cells fated to die early in embryogenesis can be eliminated by either canonical caspase-dependent apoptosis or by caspase-independent shedding.

To identify factors required for cell shedding, we tested genes involved in different cell-death processes and found that the generation of *ced-3* shed cells did not require genes that mediate germline apoptosis, cell-corpse engulfment, necrosis, autophagy or *lin-24*-mediated cell death (Supplemental Tables S1 and S3). We therefore developed a screening strategy based on the hypothesis that the shed cell ABplpappap might survive and adopt a fate associated with a lineally related cell in animals doubly defective in the canonical cell-death pathway and cell shedding. The sister cell of ABplpappap generates the neuron RMEV and the excretory cell (Fig. 3a), which functions in osmoregulation[13]. We generated a *pgp-12::cNLS::gfp* transgene to express GFP specifically in the excretory cell and observed that wild-type and *ced-3* animals contained a single GFP-positive cell (Figs. 3b and d). Using this reporter, we screened mutagenized *ced-3* animals and identified mutants with a "Tex" (two excretory cells) phenotype. Two such Tex isolates, *n5433* and *n5437*, are alleles of the gene *pig-1* (Supplemental Fig. S4). Single mutants defective in a null allele of *pig-1*, *gm344*Δ, had one excretory cell (Fig. 3d), whereas 89% of *pig-1(gm344) ced-3(n3692)* mutants contained two GFP-positive nuclei that resembled the large nucleus of the excretory cell (Figs. 3c–d; Supplemental Fig. S4). Double mutants with *pig-1* and *ced-4*, *ced-9(gf)* or *egl-1* mutations were similar to *pig-1 ced-3* animals (Supplemental Table S4). Inactivation of *pig-1* by RNAi treatment phenocopied *gm344*, *n5433* and *n5437*, confirming that loss of *pig-1* function caused the Tex phenotype in these mutants (Supplemental Table S7).

The LIN-3 EGF ligand is expressed embryonically by the excretory cell[14], and *pig-1 ced-3* embryos contained an extra cell that expressed *lin-3* (Supplemental Fig. S5a). Furthermore, the heads of *pig-1 ced-3* animals contained large cysts (Fig. 3e) similar to those of mutants with defective excretory cell function[13]. Thus, *pig-1 ced-3* mutants generated an ectopic excretory cell, albeit one that either was defective in osmoregulation or interfered with the function of the endogenous excretory cell.

To address whether the ectopic excretory cell of *pig-1 ced-3* animals is derived from the unshed ABplpappap cell, we directly examined the fate of ABplpappap in *pig-1* and *pig-1 ced-3* embryos (Supplemental Movies S2 and S3). In *pig-1* embryos (as in the wild-type), ABplpappap became a highly refractile cell corpse within 45 min of its generation (Fig. 3f and data not shown). By contrast, ABplpappap survived and divided approximately 115 min after it was generated in *pig-1 ced-3* embryos (Fig. 3g). In the three *pig-1 ced-3* embryos we examined, neither ABplpappap nor its descendants detached from the embryo, suggesting that an ABplpappap descendant gives rise to the ectopic excretory cell in *pig-1 ced-3* larvae. As previously reported[15], *pig-1 ced-3* animals also contain ectopic RME-like neurons (Supplemental Fig. S5b; Supplemental Table S5), suggesting that when ABplpappap survives it generates both an ectopic RME-like and an ectopic excretory-like cell.

pig-1 inactivation by mutation or RNAi treatment reduced the number of shed cells in *ced-3*, *ced-4* or *ced-9(gf)* embryos by nearly 75% ($p < 5.0\times10^{-7}$ for each pair-wise comparison, Student's t-test; Fig. 3h and data not shown), demonstrating that *pig-1* is generally required for the generation of shed cells. Given this observation, the effects of *pig-1* on cell shedding are in several ways comparable to the effects of *ced-3* on programmed cell death: (1) *ced-3* affects most programmed cell deaths and *pig-1* similarly affects most shed cells, indicating that *ced-3* and *pig-1* act generally to drive programmed cell death and generate shed cells, respectively; (2) like programmed cell deaths, extruded cells share morphologic and genetic properties and can be viewed as expressing a specific cell fate; and, (3) like mutations in *ced-3*, mutations in *pig-1* cause cells that should die to expresss the fates of cells that normally survive.

pig-1 encodes a homolog of MELK, an AMPK-related serine-threonine kinase required cell autonomously for the asymmetric cell divisions of many *C. elegans* neuroblasts[15,16]. Mammalian AMPK-related kinases control metabolism and cell polarity[17] and are activated via phosphorylation of a conserved threonine within their T-Loop domains by the kinase LKB1[18] and its complex partners STRADα and MO25α[19,20]. The PIG-1 T-Loop threonine (T169) was necessary for a *pig-1* transgene to rescue the ectopic excretory cell defect of *pig-1 ced-3* mutants, whereas changing T169 to a phosphomimetic aspartic acid bypassed this requirement (Fig. 3i), indicating that PIG-1 likely is activated by phosphorylation of its T-Loop. We therefore tested the *C. elegans* homologs of *LKB1*, *STRADα* and *MO25α* (*par-4*, *strd-1*, and paralogs *mop-25.1*, *mop-25.2* and *mop-25.3*, respectively) for roles in the elimination of ABplpappap. *par-4* or *strd-1* inactivation caused the Tex phenotype in *ced-3* mutants (Figs. 3j and k; Supplemental Table S6). Furthermore, the *ok2283* deletion allele of *strd-1* reduced the number of shed cells in *ced-3* embryos by 67% ($p = 1.9\times10^{-10}$, Student's t-test; Fig. 3h). The inactivation of both *mop-25.1* and *mop-25.2* was necessary to cause the Tex defect in *ced-3* mutants (Fig. 3l; Supplemental Table S6), indicating redundant function. We conclude that both PIG-1 and the PAR-4:STRD-1:MOP-25 complex are required for cell shedding in *C. elegans*.

Our genetic analyses suggest that PIG-1 and PAR-4 function in the same pathway. The deletion mutation *ok2283*, a putative null allele of *strd-1* (Supplementary Table S8), failed to enhance any of the *pig-1* or *pig-1 ced-3* defects (Fig. 4h and i; Supplementary Fig. S6; Supplementary Tables S8–9). Although, *par-4* and *strd-1* can act independently[21], this result argues that PIG-1 and PAR-4 and its binding partners function in the same pathway. We believe that PIG-1 is the phosphorylation target of PAR-4 in cell shedding because inactivation of PIG-1 but of no other AMPK-related kinase caused the survival of ABplpappap in *ced-3* mutants (Supplementary Table S7). The Tex defect of *pig-1(gm344) ced-3(n3692)* animals (89%) was higher than that of *strd-1(ok2283); ced-3(n3692)* animals (43%) (Figs. 3d; Supplementary Table S4). Thus, STRD-1 and possibly the entire PAR-4 complex are required partially for PIG-1 activation, indicating that other factors, or PIG-1 itself via autophosphorylation, also stimulate PIG-1 activity. Indeed, MELK phosphorylates itself *in vitro*[18].

How might PIG-1 regulate cell shedding? We reasoned that shed cells must be deficient in adhesive contacts with the embryo and explored whether *pig-1* modulates cell-adhesion

complexes, specifically adherens junctions. In *C. elegans*, adherens junctions comprise a cadherin-catenin complex and a complex including DLG-1 (Discs Large) and AJM-1. Both complexes participate in the enclosure of the embryo within a layer of epidermal cells[22], a major morphogenic event that coincides with the detachment of shed cells.

We examined the expression of AJM-1, DLG-1, HMP-1 (α-catenin) and JAC-1 (p120 catenin) fused to GFP in shed cells. AJM-1, DLG-1 and HMP-1 were not visible at the surface of *ced-3* or *ced-4* shed cells that had recently detached from either the anterior sensory depression (Figs. 4a and c; Supplemental Fig. S7b) or the ventral cleft (Fig. 4b; Supplemental Fig. S7a). (JAC-1::GFP was detectable in some shed cells; Supplemental Fig. S7c). The absence of cell-adhesion proteins was striking given their presence on adjacent epidermal cells (Figs. 4a–c; Supplemental Fig. S7). ABplpappap in *ced-3* embryos remained at the ventral surface of the embryo from its generation until its detachment and never expressed HMP-1::GFP (Figs. 4d and e; data not shown). By contrast, in *pig-1 ced-3* embryos, ABplpappap ingressed dorsally during ventral enclosure (Fig. 4f), matching the movement of the excretory cell away from the ventral surface[14]. Strikingly, ABplpappap and its descendants exhibited a uniform expression of HMP-1::GFP at the cell surface (Fig. 4g), indicating that a loss of *pig-1* function results in the inappropriate expression of cell-adhesion molecules. Thus, PIG-1 might facilitate cell shedding by preventing the expression of cell-adhesion molecules on the surfaces of shed cells.

Several lines of evidence suggest that *pig-1* promotes shed cell detachment through endocytosis. Many cell corpses, including the ABplpappap corpse, were not efficiently cleared in *pig-1* embryos (Figs. 4h and i). The *pig-1* cell corpses were encircled rapidly by the engulfment receptor CED-1 and stained positively with acridine orange, a marker of internalized corpses (Fig. 4j; Supplemental Fig. S8). These results demonstrate that the delay in clearance was post-engulfment and reflected a defect in corpse degradation, a process that requires endocytic pathway components[23]. Interestingly, a recent study showed that two *C. elegans* ARF GTPase genes, *arf-1.2* and *arf-6*, and an ARF GTPase-activating protein (GAP) gene, *cnt-2*, have functions in cell-fate determination similar to those of *pig-1* as well as roles in receptor-mediated endocytosis[24]. Mammalian Arf GTPases function in endocytosis[25] and can remove cadherin complexes from the cell surface[26]. We noted that inactivation of Arf GTPase genes *arf-1.2* or *arf-3* or Arf guanine exchange factor gene *grp-1* also produced ectopic excretory cells in *ced-3* mutants (Fig. 4k; Supplemental Table S10).

Taken together, our observations suggest that the PAR-4 complex, PIG-1, and ARF GTPases promote the detachment of shed cells through the endocytosis-mediated removal of cell-adhesion molecules from the cell surface. Thus, the programmed elimination and apoptosis of at least eight *C. elegans* cells can be accomplished either through canonical caspase-mediated apoptosis involving the engulfment of dying cells or through a caspase-independent shedding mechanism that also results in apoptosis and that requires the PAR-4 complex and the AMPK-related kinase PIG-1 (Fig. 3m). These two mechanisms are functionally redundant, as ABplpappap and the other shed cells survive only in mutants in which both pathways are disrupted.

We propose that cell-shedding is an evolutionarily conserved mechanism of cell elimination. Many epithelia extrude cells constitutively to maintain tissue homeostasis, and the shed epithelial cells of vertebrates share features with the shed cells of caspase-deficient *C. elegans* embryos. First, like other shed epithelial cells[4], shed intestinal enterocytes frequently exhibit apoptotic markers[27,28], including caspase-3 activation and TUNEL-reactivity. Second, despite the apoptotic appearance of shed enterocytes, the intestinal epithelia of *caspase-3*$^{-/-}$, *Apaf-1*$^{-/-}$, *bax*$^{-/-}$, *bak*$^{-/-}$, or *bcl-2* over-expressing mice are not grossly abnormal[3,29], suggesting that cell extrusion is not dependent on caspase-mediated cell-killing. Third, *LKB1* mutations cause Peutz-Jeghers syndrome (PJS)[30], which is characterized by intestinal hamartomas (polyps) containing excess epithelial cells. It is possible that *LKB1* mutations contribute to polyp formation by causing a defect in the extrusion of epithelial cells. Based on our observations of *C. elegans*, we predict that the PIG-1 homolog MELK could be a target of LKB1 in the gastrointestinal tract and that mutations of *MELK* might also impair enterocyte shedding and cause a polyposis phenotype in the mammalian intestine.

Full Methods

Strains

All *C. elegans* strains were cultured as described previously[31] and maintained at 20°C unless noted otherwise. We used the Bristol strain N2 as the wild-type strain. The mutations used in our experiments are listed below:

LGI: *ced-1(e1735), cep-1(gk138), csp-3(n4872), dapk-1(gk219), gpb-2(ad541), lin-35(n745), nIs433[*P$_{pgp-12}$*::gfp, unc-76(+)]*.

LGII: *cad-1(j1), csp-1(n4967), mop-25.2(ok2073).*

LGIII: *arf-1.2(ok796), ced-4(n1162), ced-6(n1813), ced-7(n1892), ced-9(n1950, n1950 n2077), ced-12(n3261), grp-1(tm1956), strd-1(ok2283), nIs400[*P$_{ced-1}$*::ced-1ΔC::gfp,* P$_{myo-2}$*::dsRed]*.

LGIV: *ced-2(e1752), ced-3(n717, n2452, n3692), ced-5(n1812), ced-10(n1993), csp-2(n4871), ham-1(n1438), lin-24(n4294), lin-33(n4514), pig-1(gm344, n5433, n5437), jcIs1[ajm-1::gfp, rol-6(su1006)]*.

LGV: *unc-76(e911), par-4(it57), egl-1(n1084 n3082, n3330), crt-1(ok948), unc-68(e540), unc-51(e369), nIs342[*P$_{egl-1}$*::gfp, lin-15(+)]*.

LGX: *nuc-1(e1392), lin-15AB(n765), nIs434[*P$_{pgp-12}$*::gfp, unc-76(+)]*.

unknown linkage: *nIs398[*P$_{dyn-1}$*::mfg-e8::Venus,* P$_{myo-2}$*::dsRed], jcIs17[hmp-1::gfp, dlg-1::dsRed, rol-6(su1006)], nIs201[*P$_{unc-25}$*::4xNLS::mStrawberry, plin-15EK], xnIs17[dlg-1::gfp, rol-6(su1006)], syIs107[lin-3::gfp], jcIs25[*P$_{hmr-1}$*::jac-1::gfp::unc-54(3'UTR), rol-6(su1006)]*.

Extrachromosomal arrays: *nEx1747*, *nEx1748*, and *nEx1749 [pig-1(wt),* P$_{pgp-12}$*::gfp,* P$_{myo-2}$*::dsRed]*; *nEx1758*, *nEx1759*, and *nEx1760 [pig-1(STOP),* P$_{pgp-12}$*::gfp,* P$_{myo-2}$*::dsRed]*; *nEx1755*, *nEx1756*, and *nEx1757 [pig-1(T169A),* P$_{pgp-12}$*::gfp,*

P_{myo-2}*::dsRed]*; *nEx1831*, *nEx1832*, *nEx1833*, and *nEx1834 [pig-1(T169D),* P_{pgp-12}*::gfp,* P_{myo-2}*::dsRed]*.

Plasmids

The P_{egl-1}*::gfp* transcriptional reporter and the P_{dyn-1}*::mfg-e8::Venus* (pVV59) translation reporter have been described previously[32,33]. The P_{unc-25}*::mStrawberry* transcriptional reporter (pSN223) was constructed using PCR to amplify a 1.8 kb fragment of the *unc-25* promoter region with the primers 5'-CGAATTTTTGCATGCAAAAAACACCCACTTTTTGATC and 5'-CGGGATCCTCGAGCACAGCATCACTTTCGTCAGCAGC. The resulting amplicon was digested with SphI and BamHI and ligated into pSN199, which encodes the 4xNLS::mStrawberry fusion. pSN199 was constructed by replacing the AgeI-EcoRI fragment of pPD122.56 with the AgeI-EcoRI fragment from the plasmid mStrawberry 6. The transcriptional reporter P_{pgp-12}*::gfp* (pSN359) was constructed using PCR to amplify a 2.9 kb fragment of the *pgp-12* promoter region with the primers 5'-GCAAGCTTGTGCTTGCAGTGAACCAGAAACT and 5'-CCTCTAGAATTCCATCAATTGGCTCGATCGCA. The resulting amplicon was digested with HindIII and XbaI and ligated into pPD122.56. The *pig-1* rescuing construct (pDD078) was constructed using PCR to amplify three overlapping genomic fragments spanning 17.5 kb with the following primer pairs: 5'-CAGTGAGCGCGCGTAATACGACTCACTATAGGGCGAATTGGCCACATCAAATGAAAGACG and 5'-TCAGAGTTCAATATATGTTGG; 5'-TGTCTACACCACTCCAAACACC and 5'-ACGACGGCATCAGATATTCG; and, 5'-CCAAGCGCGCAATTAACCCTCACTAAAGGGAACAAAAGCTTGATGATGATGTCCGTGAGC and 5'-CATGTCCAACAATGGAATCG. The resulting amplicons were ligated into pRS426 by homologous recombination in *Saccharomyces cerevisiae* (yeast-mediated ligation). The *pig-1(STOP)* (pDD084), *pig-1(T169A)* (pDD085) and *pig-1(T169D)* (pDD088) constructs were also genetrated by yeast-mediated ligation using a SfoI-NaeI digested fragment of pDD078. *pig-1(STOP)* changes codons 8 and 9 to the stop codons TAG and TGA, respectively. *pig-1(T169A)* changes the T-Loop threonine codon at position 169 to GCG, which encodes an alanine residue. *pig-1(T169D)* changes the T-Loop threonine codon at position 169 to GAC, which encodes an aspartic acid residue. pDD073 (pL4440::*par-4*) was constructed using PCR to amplify the *par-4* cDNA with the following primers: 5'-GCGCCGCGGATGGATGCTCCGTCGACATCC and 5'-GCGTCTAGACTAAGCACTATCGGTACGAG. The resulting amplicon was digested with SacII and XbaI and then ligated into pL4440.

Shed cell, excretory cell, persistent corpse and extra pharyngeal cell counts

Shed cells or floaters were counted in eggs between the 2-fold and 3.5-fold stages of development (approximately 450 to 600 min after the first cell division) using a 100× objective equipped with Nomarski differential interference contrast (DIC) optics. The number of excretory cells and excretory-like cells were counted in L3 larvae carrying the P_{pgp-12}*::gfp* transcriptional reporter using a 100× objective. A cell was scored as an excretory cell if it was located in the anterior third of the animal and its nucleus strongly

expressed GFP. Persistent cell corpse and extra pharyngeal cell counts were performed as described previously[34].

Mutagenesis screen for synTex mutants

ced-3(n3692); nIs434 or *nIs433; ced-3(n3692)* L4 larvae were mutagenized with ethyl methanesulfonate (EMS) as described previously[31]. Using a dissecting microscope equipped for the detection of GFP fluorescence, we screened approximately 25,000 F3 progeny of the mutagenized animals for an extra GFP+ cell near the posterior bulb of the pharynx. We showed by complementation testing and DNA sequence determination that two of the mutants isolated from this screen, *n5433* and *n5437*, were alleles of *pig-1*.

RNAi treatments

RNAi treatments were performed by feeding using RNAi constructs and reagents described previously[35,36]. Briefly, HT115 *E. coli* carrying RNAi clones in the pL4440 vector were cultured overnight in LB liquid media with antibiotics. NGM plates containing 1 mM IPTG and antibiotics were seeded with the LB culture and incubated 24 hrs at 20°C. Five L2 larvae were placed onto each seeded NGM plate, and the progeny of these animals were scored for either shed cells or ectopic excretory cells as described above. Control RNAi treatments were performed with the empty vector pL4440. The complete sequences of all RNAi sequences used in this study are provided in the Supporting Information.

TUNEL and acridine orange staining

Terminal deoxynucleotidyl transferase dUTP nick end labeling (TUNEL) reactions were performed as described previously[37,38]. Fixation times (between 12 and 16 min) were optimized for labeling the floaters in *ced-5(n1812); nuc-1(e1392)* eggs. *nuc-1(e1392)* facilitates the observation of TUNEL-reactivity. Acridine orange staining of embryos was performed as described previously[39].

Transmission electron microscopy

Gravid *sem-4(n1378); ced-5(n1812)* or *sem-4(n1971); ced-3(n717)* adult animals were fixed by high pressure freezing in an HPM010 high pressure freezer by Abra. They were then substituted using an RMC FS-7500 freeze substitution system with 2% osmium, 2% water in acetone at −90°C for 5 days, warmed to −20°C over 14 hours, and then held at −20°C for 16 hrs before warming to 0°C. Samples were washed 6 × 20 min, infiltrated stepwise into Eponate 12 resin (Ted Pella), and polymerized at 60°C. The resulting blocks were sectioned at 50 nm, post stained with uranyl acetate and lead, and imaged with a JEM-1200EX II microscope (Jeol) using an AMT XR41 CCD camera. *sem-4* mutations cause eggs to accumulate in the hermaphrodite gonad, allowing more embryos (including more later-stage embryos) to be analyzed per sample.

Microscopy

Nomarski DIC and epifluorescence micrographs were obtained using an Axioskop II (Zeiss) compound microscope and OpenLab software (Agilent). Merged DIC and epifluorescence images were generated using ImageJ software (NIH). For the time-lapse experiments, early

(2 or 4-cell stage) embryos were dissected from gravid adults, mounted on a slide with a 4% agar pad, and covered with a coverslip that was sealed to the slide with petroleum jelly to prevent the preparation from drying. The developing embryos were imaged every four minutes for a total of 300 min, and at each time point a Z-stack of 50 images spaced at 0.6 μm was acquired. Confocal microscopy was performed using a Zeiss LSM 510 instrument, and the resulting images were prepared and modified using ImageJ software.

Supplementary Material

Refer to Web version on PubMed Central for supplementary material.

Acknowledgements

We thank Z. Zhou, T. Hirose and S. Nakano for reporter constructs; B. Castor, E. Murphy and R. Droste for determining DNA sequences; S. Dennis for screening of the deletion library; N. An for strain management; and, J. Yuan, S. Nakano, N. Paquin, C. Engert and A. Saffer for helpful discussions. The *Caenorhabditis* Genetic Center, which is funded by the NIH National Center for Research Resources (NCRR), provided many strains. S. Mitani kindly provided *grp-1(tm1956)*. D.P.D. was supported by postdoctoral fellowships from the Damon Runyon Cancer Research Foundation and from the Charles A. King Trust. H.R.H. is the David H. Koch Professor of Biology at the Massachusetts Institute of Technology and an Investigator of the Howard Hughes Medical Institute.

References

1. Fuchs Y, Steller H. Programmed cell death in animal development and disease. Cell. 2011; 147:742–758. [PubMed: 22078876]
2. Reddien PW, Horvitz HR. The engulfment process of programmed cell death in *Caenorhabditis elegans*. Annu. Rev. Cell Dev. Biol. 2004; 20:193–221. [PubMed: 15473839]
3. Yuan J, Kroemer G. Alternative cell death mechanisms in development and beyond. Genes Dev. 2010; 24:2592–2602. [PubMed: 21123646]
4. Rosenblatt J, Raff MC, Cramer LP. An epithelial cell destined for apoptosis signals its neighbors to extrude it by an actin- and myosin-dependent mechanism. Curr. Biol. 2001; 11:1847–1857. [PubMed: 11728307]
5. Ellis HM, Horvitz HR. Genetic control of programmed cell death in the nematode *C. elegans*. Cell. 1986; 44:817–829. [PubMed: 3955651]
6. Abraham MC, Lu Y, Shaham S. A morphologically conserved nonapoptotic program promotes linker cell death in *Caenorhabditis elegans*. Dev. Cell. 2007; 12:73–86. [PubMed: 17199042]
7. Shaham S, Reddien PW, Davies B, Horvitz HR. Mutational analysis of the *Caenorhabditis elegans* cell-death gene *ced-3*. Genetics. 1999; 153:1655–1671. [PubMed: 10581274]
8. Wu YC, Stanfield GM, Horvitz HR. NUC-1, a *Caenorhabditis elegans* DNase II homolog, functions in an intermediate step of DNA degradation during apoptosis. Genes Dev. 2000; 14:536–548. [PubMed: 10716942]
9. Shaham S. Identification of multiple *Caenorhabditis elegans* caspases and their potential roles in proteolytic cascades. J. Biol. Chem. 1998; 273:35109–35117. [PubMed: 9857046]
10. Sulston JE, Horvitz HR. Post-embryonic cell lineages of the nematode *Caenorhabditis elegans*. Dev. Biol. 1977; 56:110–156. [PubMed: 838129]
11. Sulston JE, Schierenberg E, White JG, Thomson JN. The embryonic cell lineage of the nematode *Caenorhabditis elegans*. Dev. Biol. 1983; 100:64–119. [PubMed: 6684600]
12. Potts MB, Cameron S. Cell lineage and cell death: *Caenorhabditis elegans* and cancer research. Nat. Rev. Cancer. 2011; 11:50–58. [PubMed: 21150934]
13. Buechner M. Tubes and the single *C. elegans* excretory cell. Trends Cell Biol. 2002; 12:479–484. [PubMed: 12441252]
14. Abdus-Saboor I, et al. Notch and Ras promote sequential steps of excretory tube development in *C. elegans*. Development. 2011; 138:3545–3555. [PubMed: 21771815]

15. Cordes S, Frank CA, Garriga G. The *C. elegans* MELK ortholog PIG-1 regulates cell size asymmetry and daughter cell fate in asymmetric neuroblast divisions. Development. 2006; 133:2747–2756. [PubMed: 16774992]
16. Ou G, Stuurman N, D'Ambrosio M, Vale RD. Polarized myosin produces unequal-size daughters during asymmetric cell division. Science. 2010; 330:677–680. [PubMed: 20929735]
17. Shackelford DB, Shaw RJ. The LKB1-AMPK pathway: metabolism and growth control in tumour suppression. Nat. Rev. Cancer. 2009; 9:563–575. [PubMed: 19629071]
18. Lizcano JM, et al. LKB1 is a master kinase that activates 13 kinases of the AMPK subfamily, including MARK/PAR-1. EMBO J. 2004; 23:833–843. [PubMed: 14976552]
19. Boudeau J, et al. MO25alpha/beta interact with STRADalpha/beta enhancing their ability to bind, activate and localize LKB1 in the cytoplasm. EMBO J. 2003; 22:5102–5114. [PubMed: 14517248]
20. Zeqiraj E, Filippi BM, Deak M, Alessi DR, van Aalten DMF. Structure of the LKB1-STRAD-MO25 complex reveals an allosteric mechanism of kinase activation. Science. 2009; 326:1707–1711. [PubMed: 19892943]
21. Narbonne P, Hyenne V, Li S, Labbé J-C, Roy R. Differential requirements for STRAD in LKB1-dependent functions in *C. elegans*. Development. 2010; 137:661–670. [PubMed: 20110331]
22. Labouesse M. Epithelial junctions and attachments. WormBook. 2006:1–21. [PubMed: 18050482]
23. Kinchen JM, et al. A pathway for phagosome maturation during engulfment of apoptotic cells. Nat. Cell Biol. 2008; 10:556–566. [PubMed: 18425118]
24. Singhvi A, et al. The Arf GAP CNT-2 regulates the apoptotic fate in *C. elegans* asymmetric neuroblast divisions. Curr. Biol. 2011; 21:948–954. [PubMed: 21596567]
25. D'Souza-Schorey C, Chavrier P. ARF proteins: roles in membrane traffic and beyond. Nat. Rev. Mol. Cell Biol. 2006; 7:347–358. [PubMed: 16633337]
26. D'Souza-Schorey C. Disassembling adherens junctions: breaking up is hard to do. Trends Cell Biol. 2005; 15:19–26. [PubMed: 15653074]
27. Potten CS. Stem cells in gastrointestinal epithelium: numbers, characteristics and death. Philos. Trans. R. Soc. Lond., B, Biol. Sci. 1998; 353:821–830. [PubMed: 9684279]
28. Watson AJM, Duckworth CA, Guan Y, Montrose MH. Mechanisms of epithelial cell shedding in the mammalian intestine and maintenance of barrier function. Ann. N.Y. Acad. Sci. 2009; 1165:135–142. [PubMed: 19538298]
29. Coopersmith CM, O'Donnell D, Gordon JI. Bcl-2 inhibits ischemia-reperfusion-induced apoptosis in the intestinal epithelium of transgenic mice. Am. J. Physiol. 1999; 276:G677–G686. [PubMed: 10070044]
30. Hemminki A, et al. A serine/threonine kinase gene defective in Peutz-Jeghers syndrome. Nature. 1998; 391:184–187. [PubMed: 9428765]

Methods References

31. Brenner S. The genetics of *Caenorhabditis elegans*. Genetics. 1974; 77:71–94. [PubMed: 4366476]
32. Hirose T, Galvin BD, Horvitz HR. Six and Eya promote apoptosis through direct transcriptional activation of the proapoptotic BH3-only gene *egl-1* in *Caenorhabditis elegans*. Proc. Natl. Acad. Sci. U.S.A. 2010; 107:15479–15484. [PubMed: 20713707]
33. Venegas V, Zhou Z. Two alternative mechanisms that regulate the presentation of apoptotic cell engulfment signal in *Caenorhabditis elegans*. Mol. Biol. Cell. 2007; 18:3180–3192. [PubMed: 17567952]
34. Schwartz HT. A protocol describing pharynx counts and a review of other assays of apoptotic cell death in the nematode worm *Caenorhabditis elegans*. Nat Protoc. 2007; 2:705–714. [PubMed: 17406633]
35. Fraser AG, et al. Functional genomic analysis of *C. elegans* chromosome I by systematic RNA interference. Nature. 2000; 408:325–330. [PubMed: 11099033]

36. Rual JF, et al. Toward improving *Caenorhabditis elegans* phenome mapping with an ORFeome-based RNAi library. Genome Res. 2004; 14:2162–2168. [PubMed: 15489339]

37. Wu YC, Stanfield GM, Horvitz HR. NUC-1, a *Caenorhabditis elegans* DNase II homolog, functions in an intermediate step of DNA degradation during apoptosis. Genes Dev. 2000; 14:536–548. [PubMed: 10716942]

38. Parrish JZ, Xue D. Functional genomic analysis of apoptotic DNA degradation in *C. elegans*. Mol. Cell. 2003; 11:987–996. [PubMed: 12718884]

39. Lu Q, et al. C. elegans Rab GTPase 2 is required for the degradation of apoptotic cells. Development. 2008; 135:1069–1080. [PubMed: 18256195]

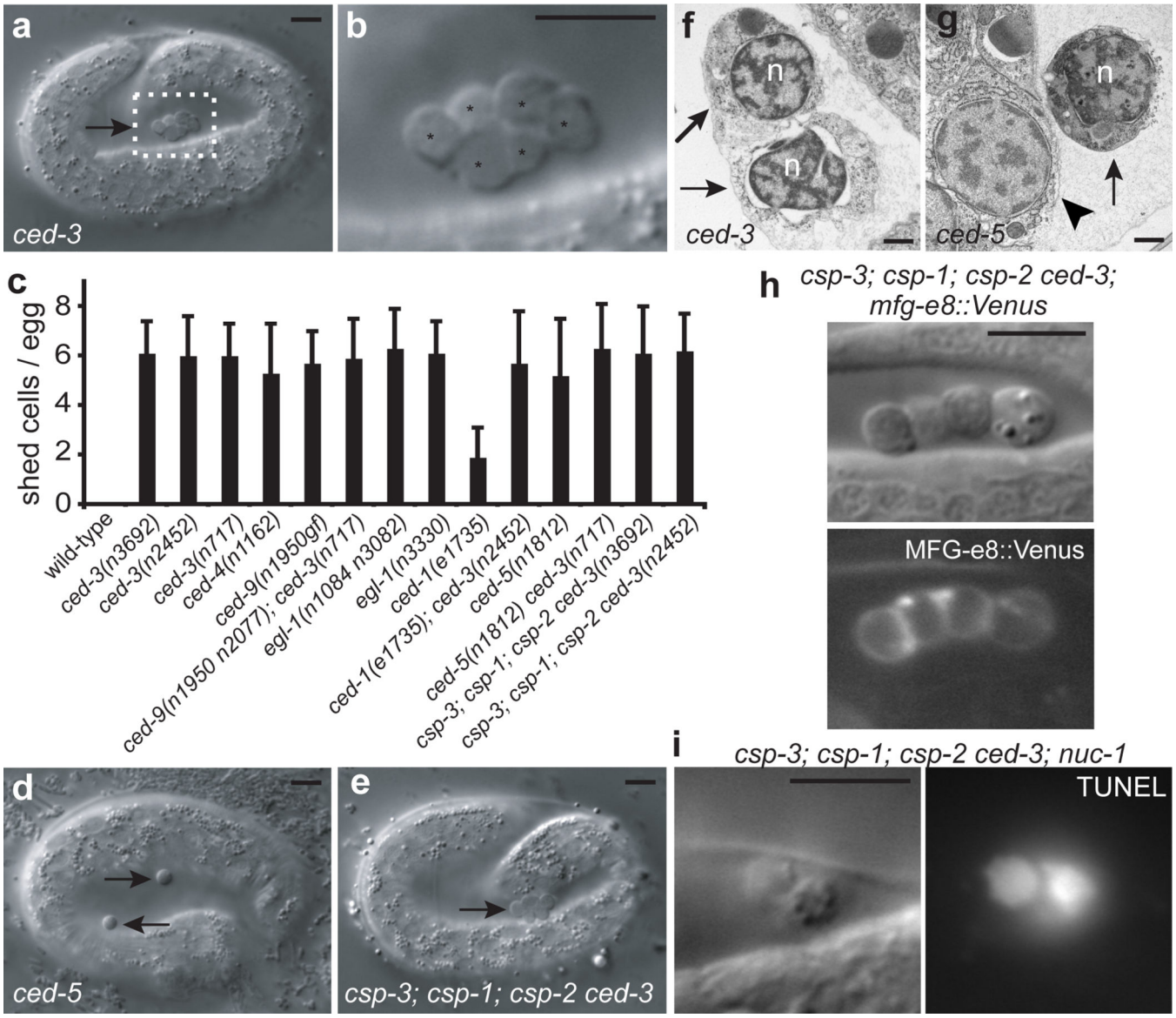

Figure 1.

Cells with apoptotic morphology are shed from *C. elegans* embryos lacking caspase activity. **(a, b)** (a) Low and (b) high magnification differential interference contrast (DIC) images of a *ced-3(n3692)* egg with a cluster of six cells that detached from the embryo. Asterisks, individual shed cells in (b). **(c)** Quantification of shed cells or floaters in mutants defective in programmed cell death and/or corpse engulfment. Error bars, s.d. **(d)** A *ced-5(n1812)* egg with two floaters. **(e)** A *csp-3; csp-1; csp-2 ced-3* egg with a cluster of five shed cells. **(f, g)** Transmission electron micrographs of shed cells from (f) *ced-3(n717)* and (g) *ced-5(n1812)* embryos. Arrows, shed cells; arrowhead, an embryonic cell in (g); n, nucleus. **(h)** The phosphatidylserine binding protein MFG-e8 expressed from the transgene *nIs398[*$P_{dyn\text{-}1}$*::mfge8::Venus]* associates with the surface of *csp*-Δ shed cells. **(i)** The shed cells of *csp*-Δ*; nuc-1(e1392)* eggs are TUNEL-reactive. Scale bars, 10 μm.

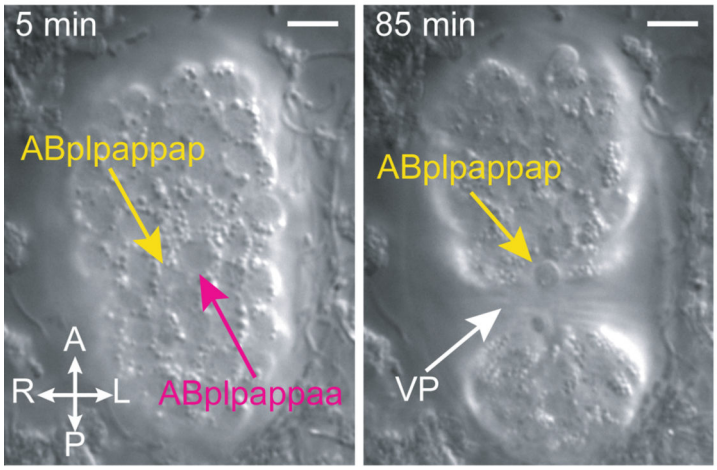

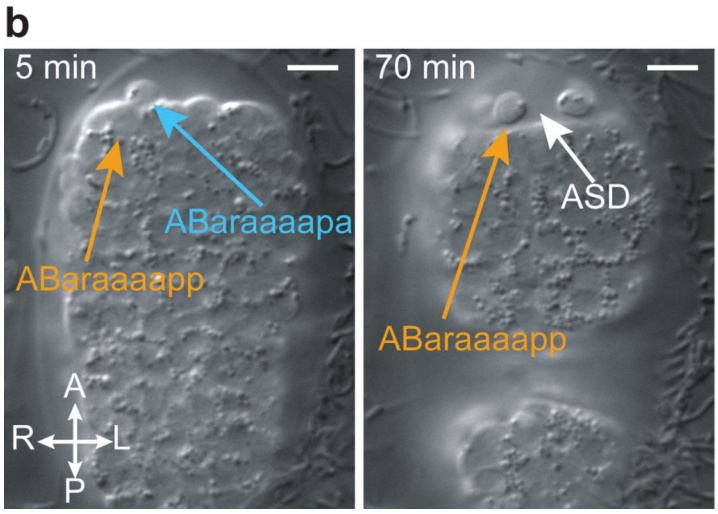

c

shed cell ID	location at detachment	t (min) post fert. of death in wild type
ABalapapaa*	VP	250
ABplpappap	VP	250
ABalppaaaa	ASD	275
ABalppaapa	ASD	275
ABaraaaapp	ASD	275
ABplppaaap	VP	275
ABplpppapp	VP	275
ABalpapappa	ASD	325

* Reported in ref. 5
VP = ventral pocket
ASD = anterior sensory depression

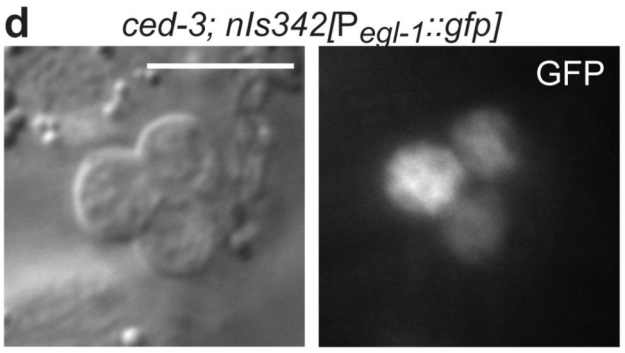

Figure 2.

The cells that are shed from *ced-3* embryos are normally fated to die early during wild-type embryogenesis. **(a, b)** DIC micrographs of *ced-3(n3692)* embryos showing (a) ABplpappap and (b) ABaraaaapp 5 min after generation and shortly after shedding from the embryo (85 and 70 min later, respectively); vp, ventral pocket; asd, anterior sensory depression. **(c)** Cells that can be shed from *ced-3(n3692)* embryos, their locations when extruded, and the timings of their deaths in wild-type embryos[11]. **(d)** DIC and fluorescence micrographs of shed cells from a *ced-3(n717)* embryo containing the *nIs342[*$P_{egl\text{-}1}$*::gfp]* transgene, which expresses GFP from the *egl-1* promoter. Scale bars, 10 μm.

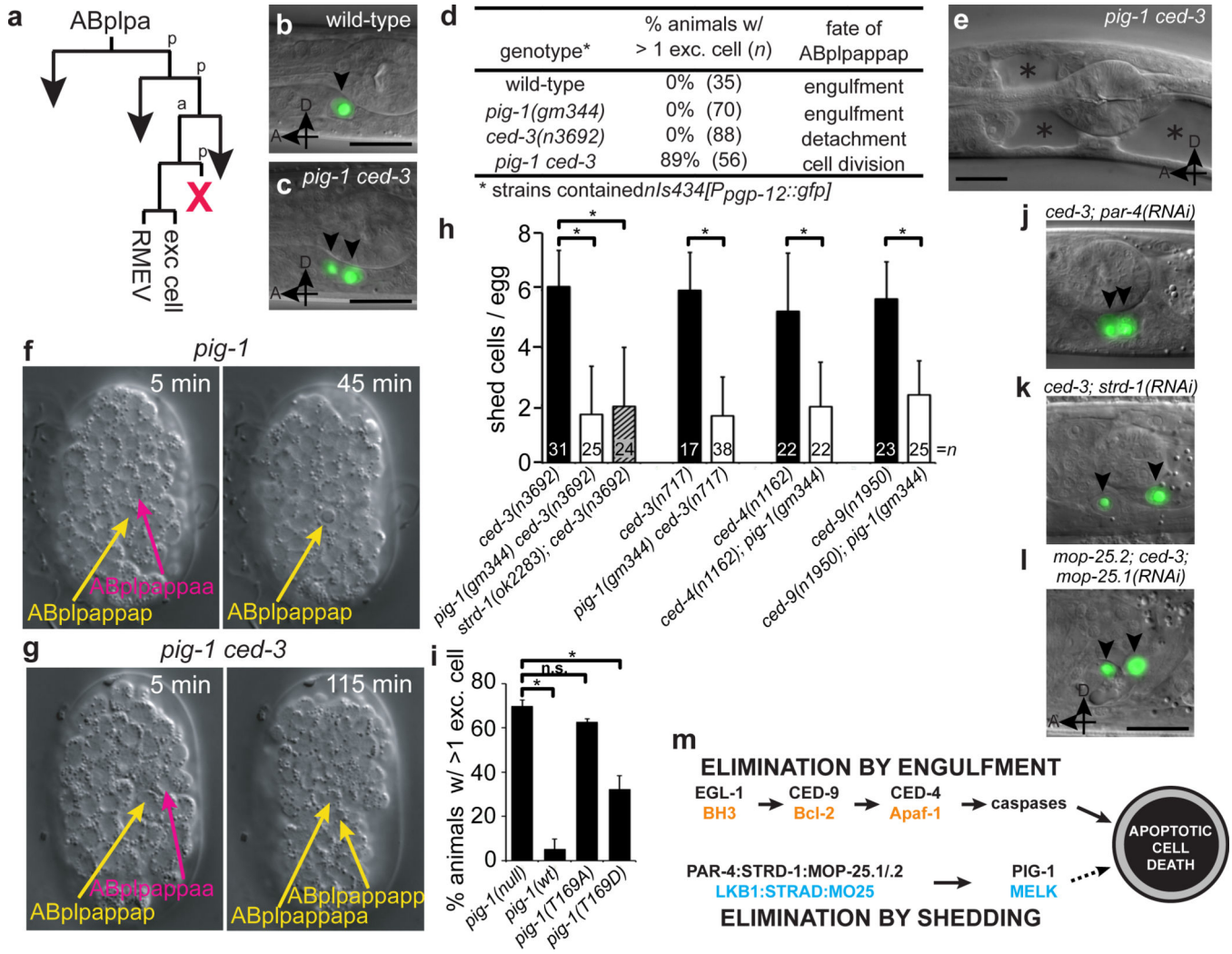

Figure 3.

The LKB1 homolog PAR-4 and the AMPK-related kinase PIG-1 are required for cell shedding from *ced-3* embryos. **(a)** The sublineage that produces the shed cell ABplpappap, which is the lineal aunt of the neuron RMEV and the excretory cell (exc cell). **(b, c)** Merged DIC and fluorescence micrographs of (b) wild-type and (c) *pig-1(gm344) ced-3(n3692)* larvae containing the transgene *nIs434[*$P_{pgp\text{-}12}$*::gfp]*, which expresses GFP in the excretory cell. Arrowheads, excretory and ectopic excretory-like cells. **(d)** Percentage of L3 larvae with ectopic excretory cells. **(e)** The head of a larval *pig-1(gm344) ced-3(n3692)* animal containing large cysts (asterisks). **(f, g)** The fate of the cell ABplpappap in *pig-1(gm344)* and *pig-1(gm344) ced-3(n3692)* embryos. (f) ABplpappap in a *pig-1* embryo shown 5 min after its generation and shortly after it underwent programmed cell death 45 min later. (g) ABplpappap in a *pig-1 ced-3* embryo shown 5 min after its generation and immediately after it divided 115 min later. **(h)** *pig-1* and *strd-1* are required for cell shedding. Mutation of *pig-1* of *strd-1* reduced the number of shed cells in *ced-3*, *ced-4* or *ced-9(gf)* eggs. Error bars, s.d.; asterisk, $p < 5\times10^{-7}$ (Student's t-test). **(i)** The T-Loop threonine (T169) of PIG-1 is required for the elimination of ABplpappap. Average percentage of larvae with ectopic

excretory cells from multiple *pig-1(gm344) ced-3(n3692)* lines carrying the following *pig-1* transgenes: *pig-1(wt)*, the wild-type *pig-1* genomic locus (three lines, n = 42, 47 and 58); *pig-1(null)*, two STOP codons in the first exon (three lines, n = 40, 43 and 45); *pig-1(T169A)*, threonine 169 changed to alanine (three lines, n = 40, 41 and 48) ; and, *pig-1(T169D)*, threonine 169 changed to aspartic acid (five lines, n = 31, 32, 43, 48 and 50); error bars, s.e.m.; asterisk, $p < 10^{-3}$; n.s., $p > 0.05$ (Student's t-test). **(j, k, l)** Merged DIC and fluorescence micrographs of (j) *ced-3(n3692); par-4(RNAi)*, (k) *ced-3(n3692); strd-1(RNAi)*, and (l) *mop-25.2(ok2073); ced-3(n3692); mop-25.1(RNAi)* larvae carrying *nIs434[*$P_{pgp\text{-}12}$*::gfp]*. Arrowheads, excretory and ectopic excretory-like cells. **(m)** Redundant pathways mediate the elimination of ABplpappap and other cells shed from *ced-3* embryos. Scale bars, 10 μm.

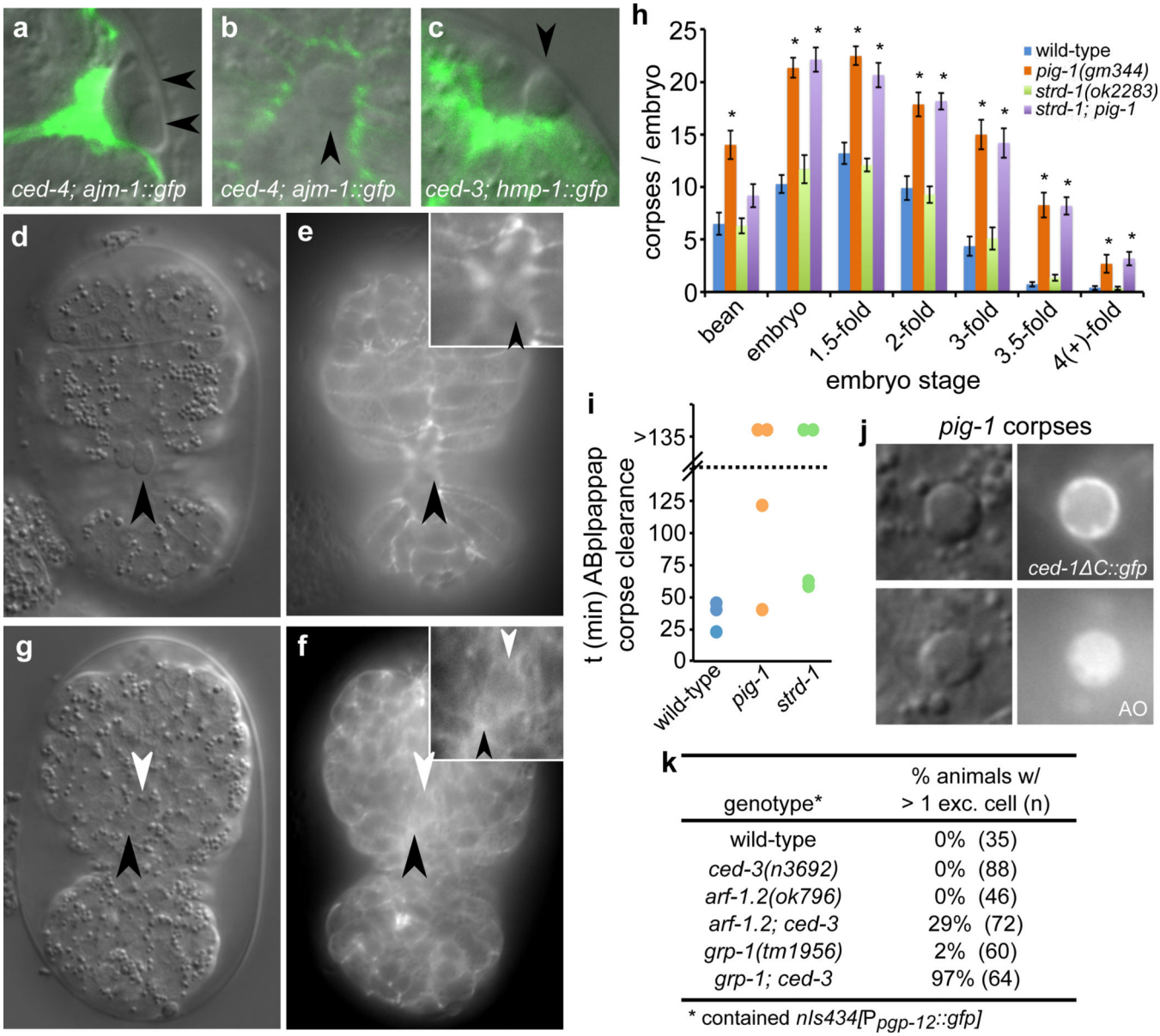

k

genotype*	% animals w/ > 1 exc. cell (n)
wild-type	0% (35)
ced-3(n3692)	0% (88)
arf-1.2(ok796)	0% (46)
arf-1.2; ced-3	29% (72)
grp-1(tm1956)	2% (60)
grp-1; ced-3	97% (64)

* contained *nIs434[P$_{pgp-12}$::gfp]*

Figure 4.

Shed cells lack cell-adhesion molecules that are inappropriately expressed in *pig-1* mutants, possibly because of impaired endocytosis. **(a, b, c)** Merged DIC and confocal fluorescence micrographs of shed cells from (a, b) *ced-4(n1162); jcIs1[ajm-1::gfp]* and (c) *ced-3(n3692); jcIs17[hmp-1::gfp]* eggs. Arrowheads, detached shed cells. **(d, e, f, g)** DIC and epifluorescence micrographs of (d, e) *ced-3(n3692); jcIs17[hmp-1::gfp]* and (f, g) *pig-1(gm344) ced-3(n3692); jcIs17[hmp-1::gfp]* embryos just prior to the completion of ventral enclosure. Black arrowheads, ABplpappap (d, e) or its descendant (f, g); white arrowhead, excretory cell (ABplpappaap); insets, magnification of ABplpappap or the excretory cell and the ABplpappap descendant in (f, g). **(h)** Number of persistent cell corpses in wild-type, *pig-1(gm344)*, *strd-1(ok2283)* and *strd-1(ok2283); pig-1(gm344)* embryos. *n* values are provided in Supplemental Table S11; error bars, s.e.m.; asterisk, $p <$

0.002 for pair-wise comparison with the wild type (Student's t-test). **(i)** Time required for engulfment and degradation of ABplpappap cell corpses in wild-type, *pig-1(gm344)* or *strd-1(ok2283)* embryos. **(j)** DIC and fluorescence micrographs of cell corpses from "bean" stage *pig-1(gm344)* embryos either carrying the *nIs400[*$P_{ced\text{-}1}$*::ced-1ΔC::gfp]* transgene or stained with acridine orange. **(k)** Percentage of L3 larvae with ectopic excretory cells.